Am J Nucl Med Mol Imaging 2012;2(2):151-162
www.ajnmmi.us /ISSN:2160-8407/ajnmmi1201002

Original Article

Multispectral visualization of surgical safety-margins using fluorescent marker seeds

Patrick TK Chin[1,*], Chantal AC Beekman[1,*], Tessa Buckle[1], Lee Josephson[2], Fijs WB van Leeuwen[1]

*[1]Department of Radiology, Interventional Molecular Imaging Section, Leiden University Medical Center (LUMC), Albinusdreef 2, 2300RC Leiden, the Netherlands; [2]Center for Molecular Imaging Research, Massachusetts General Hospital and Harvard Medical School, Building 149, 13th Street, Charlestown, MA 02129, USA. *authors contributed equally.*

Received January 23, 2012; accepted February 12, 2012; Epub March 28, 2012; Published April 15, 2012

Abstract: Optical guidance provided by luminescent marker seeds may be suitable for intraoperative determination of appropriate resection margins. In phantom studies we compared the tissue penetration of several organic dyes and inorganic particles (quantum dots; QDs) after incorporation in experimental marker seeds. The tissue penetration of (near infra-) red organic dyes was much better than the penetration of dyes and QDs with an emission in the visible range. By combining 3 dyes in a single marker seed we were able to distinguish four depth ranges. The difference in tissue penetration between the dyes and QDS enabled depth estimation via a 'traffic light' approach.

Keywords: Surgical guidance, fluorescence, tissue penetration, phantom studies, marker seeds

Introduction

A significant clinical problem in oncology is the inability to fully excise the tumor during resection leading to tumor-positive margins in for instance breast conserving surgery. Therefore, tumor-bracketing techniques based on marker seeds that help guide the surgeon towards the lesion which provide estimation of an adequate safety margin, are expected to improve the clinical outcome [1]. Since surgery is mostly a "see and treat" process, real-time optical detection is the modality of choice, in order to provide real-time guidance and verification during the process of resection. For this reason, intraoperative luminescence imaging is emerging in the surgical arena. Luminescent dyes such as fluorescein and indocyanine green (ICG) are mostly used for superficial imaging of blood flow or lymph nodes, the latter by augmenting radio-guided surgery [2-6].

Compared to radioactivity based detection techniques optical imaging suffers from a relatively high background signal and limited tissue penetration [7]. This is partly due to the requirement of an external excitation light source to elicit an emission from luminescent probes. Depending on the excitation wavelength, this results in varying background signals caused by reflectance, scattering and tissue autofluorescence [8]. In addition, tissue absorption of light results in attenuation of both excitation and emission signals, which is also wavelength dependent. As tissue absorption and autofluorescence are less prominent in the near-infrared region (NIR; 700-1000 nm), luminescent imaging agents that both absorb and emit in the NIR are preferred [9].

To extract as much information as possible from a luminescence imaging effort, multispectral imaging methodologies can be used. These methods involve capturing image data across the visible- and NIR regions of the electromagnetic spectrum, ranging between 400 and 1000 nm, and differentiating between wavelengths using band-pass filters. This technique can be used to detect multiple emissions with different wavelengths simultaneously, allowing visible emissions to be combined with (invisible) NIR emissions. Such multispectral imaging approaches can be used to increase detection specificity by isolating the signal from autofluo-

rescence [10-12]. Furthermore, the difference in tissue penetration between various emissions can be used to provide a rough estimate of the depth at which a particular luminescent marker is located in the tissue [1]. To this end either "cocktails" of dyes or multi-emissive luminescent imaging agents can be used. We previously reported on InP/ZnS quantum dots (QDs) that combine an exciton emission in the visible range (e.g. 520 nm) with a long lifetime x-ray induced defect emission at 660 nm [13]. The great advantages of QDs are their bright size tunable emission and broad absorption [14]. An efficient QD clearance from the body based on the renal filtration threshold [15, 16] is less important in a marker seed application. For a luminophore to be suitable for potential clinical marker seed applications, it has to meet several criteria: 1) high detection sensitivity at a relatively low dye concentration, using conventional imaging equipment, 2) efficient tissue penetration, i.e. excitation and emission maxima that suffer little signal absorption, 3) low signal scattering, to limit loss of resolution, and 4) little interference by background luminescence.

Previously, we showed the utility of dual emissive InP/ZnS core shell QDs in our multispectral depth estimation approach in which sequential detection of different emission colors with a different degree of tissue penetration could be used to estimate surgical safety margins [1].

Here we explore an expansion of our marker seed-based "traffic light" approach by implementing clinically approved dyes such as fluorescein and indocyanine green (ICG). The potential of dyes with varying emission wavelengths in a multi-emissive depth estimation application was compared. The possibility of accurate depth estimation using the different tissue penetrations was explored using a preclinical fluorescence scanner equipped with the standard excitation and emission filters and without the use of complex models for light propagation. In this setting we attempted to distinguish the optical properties of different excitation and emission wavelengths that may limit the use of these luminophores in vivo. Hereby we systematically and directly compared common organic dyes to dual-emissive InP/ZnS QDs [13]. By addressing the criteria mentioned above we assessed the potential of these luminophores in multi-emissive marker seeds and illustrated this by refining our safety-margin estimation approach.

Materials and methods

Dyes and nanoparticles

FITC (#F7250) and TRITC (#87918) were obtained from Sigma Aldrich (Zwijndrecht, the Netherlands). The clinical grade ICG was obtained from Pulsion Medical (Munich, Germany) and the Cy5.5 was prepared as previously described [17]. The dual emissive InP/ZnS QDs were produced as previously reported by Chin et al. [13].

Preparation of seeds

For the tissue penetration experiments, marker seeds were made out of glass capillaries, as previously reported by Buckle et al. [1]. The seeds were then filled with; A) a solution of organic dye in saline at a concentration of 0.5 mg/mL or B) a solution of dual-emissive InP/ZnS QDs (both the visible exciton fluorescence and a x-ray induced defect related emission) in 1-octadecene at 1 mg/mL or 10 mg/mL. Subsequently, seeds were closed with a small drop of epoxy resin. The dimensions of the seed were 1.0 x 5.0 mm (diameter x length).

Spectral characterization and dilution curve

Emission spectra were recorded using a spectrophotometer containing a CCD spectrometer (VS140 VIS-NIR; Horiba Jobin Yvon Inc, Edison NJ, USA) and for excitation LEDs of different wavelengths were used: 390 nm (Nichia, Tokuschima, Japan), 457 nm, 521 nm and 627 nm (Luxeon; Philips, USA) and 760 nm (Edmund Optics, York, UK). Concentration measurements and tissue penetration experiments were performed using an IVIS 200 camera (Caliper LifeSciences, Hopkinton MA, USA). For the organic dyes, standard excitation and emission filter settings were used (**Table 1**). The InP/ZnS QDs were imaged as previously reported [13] using the GFP excitation filter combined with the GFP emission filter (green QDs), or the 660 nm emission band pass filter (red QDs) (**Table 1**). The pre-illuminated defect emission of the InP/ZnS QDs was recorded using the emission open filter settings and closed excitation filters. Concentration curves were measured by imaging a black, non-fluorescent, 96-wells plate containing different concentrations between 0.1 to 1 mg/mL, in triplicate. In order to obtain signal-to-background ratios (SBR), all luminophore emis-

Table 1. IVIS 200 settings and light sources used to image the different luminophores.

	Excitation			Emission			Dye
	Source	Setting	Filter(nm)	Type	Setting	Filter(nm)	Max(nm)
FITC	IVIS	GFP	445-490	fluorescent	GFP	515-575	520
TRITC	IVIS	dsRed	500-550	fluorescent	dsRed	575-650	570
Cy5.5	IVIS	Cy5.5	615-665	fluorescent	Cy5.5	695-770	704
ICG	IVIS	ICG	705-780	fluorescent	ICG	810-885	830
Green InP/ZnS QD exciton	IVIS	GFP	445-490[$]	fluorescent	GFP	515-575	565
Green InP/ZnS QD defect	UV lamp	/	366[$]	luminescent	open filters		660
Red InP/ZnS QD exciton	IVIS	GFP	455-490	fluorescent	660	650-670	630
Red InP/ZnS QD defect	UV lamp	/	366	luminescent	open filters		720

[$]The same settings were also previously used to illuminate the InP/ZnS QDs [1, 13].

sion signals were divided by a background signal obtained from a sample of saline/1-octadecene without the luminophore, using the following formula: $SBR_{ex} = I_{seed}/I_{background}$.

Set-up and depth penetration in tissue

To determine the penetration of emissions through tissue, a marker seed was placed in the IVIS 200 chamber, on top of 4 mm of fresh tenderloin tissue. To determine the tissue penetration, the seed was covered with an increasing amount of tissue -pork tenderloin, beef sirloin, or leaf lard- until the signal could no longer be separated from the background (**Figure 1**). The tissue slices were cut at fixed thicknesses (1 mm) by an automated meat slicer. The tissue penetration depth was measured using the different spectral settings shown in **Table 1**. The tissue penetration experiments were conducted in triplicate. As "pale" pork tenderloin is not representative for all tissues encountered in clinical situations, tissue penetration of the organic dyes with the highest penetration in tenderloin (ICG and Cy5.5) was also determined in the more blood containing beef sirloin and lard (representing fat). In addition the fluorescence signals from ICG and Cy5.5 were normalized to the value measured with a bare seed placed on top of 4mm tissue.

Quantification of tissue penetration

The signal intensities were quantified using Living Image 3D software (Caliper LifeSciences, Hopkinton MA, USA). A region of interest (ROI) was selected to determine the Total Flux (photons/s/cm^2). As the illumination was quite homogeneous within the field of view, the SBR could be determined by dividing the signal from a ROI surrounding the seed by the background signal from a ROI drawn elsewhere in the same field of view.

Light scattering

To determine the scattering of the different ICG, Cy5.5 and QDs emissions, the diameter of the luminescence signal where the intensity of this signal was reduced to half its intensity maximum as a function of penetration depth through sirlion, tenderloin, and lard was measured. This parameter will be referred in the following text to as spot size at half maximum (SSHM). The SSHM specifies the minimally required distance between two sources in order to be distinguished separately. Images were analyzed using ImageJ software: A line-shaped ROI was drawn through the center of the signal and the signal intensities along this line were plotted in a profile graph. The SSHM was then determined from this graph.

Background signal of tissues

We determined the background signal in sirloin, tenderloin and lard used in our tissue penetration experiments, as well as the background measured in different mouse organs (n=5) and the standard chow used to feed the mice (irradiated AM-II chow; Abdiets #2146). The tissues were arranged on a black paper background to minimize reflections. Luminescence was measured at the wavelength ranges for $GFP_{515\text{-}575\ nm}$, $dsRed_{575\text{-}650\ nm}$, $Cy5.5_{695\text{-}770\ nm}$ and $ICG_{810\text{-}885\ nm}$ settings (**Table 1**). The signal of the

non-fluorescent black paper varied considerably when measured at these different wavelength settings, likely due to differences in illumination, spectral filtering and/or detection efficiency of the system. Therefore, fluorescent signals measured in the different tissues were divided by the signal obtained from black paper background (obtained from the same image).

Depth estimation

The difference in tissue penetration of different emissions through tenderloin tissue can be used to estimate the depth of the seed in the tissue [1]. To illustrate this, a marker seed was filled with a mixture of ICG, TRITC and FITC at 0.5 mg/mL each. The tissue penetration experiment was performed using the IVIS 200 as described above, using $ICG_{810\text{-}885\ nm}$, $dsRed_{575\text{-}650\ nm}$ and $GFP_{515\text{-}575\ nm}$ filter settings (i.e. images were taken at 3 different settings).

Results

In order to determine the value of combining different dyes in surgical guidance applications, and in particular depth-estimation approaches using multi-emissive marker seeds, were directly compared under identical conditions. Here fore, marker seeds containing the potentially interesting organic dyes, FITC, TRITC, Cy5.5 and ICG were compared to two differently sized InP/ZnS QDs [1, 13].

Organic dyes: signal vs. concentration

The brightness of the different commercially available organic luminophores was compared in order to provide an indication of the concentration (mg/mL) required for a particular imaging application. To this end the signal to background ratio (SBR) of their emissions was measured at different dye concentrations (mg/mL). FITC, TRITC, Cy5.5 and ICG were measured using the standard "GFP", "dsRed", "Cy5.5", and "ICG" settings (**Figure 1**). The different excitation filters and the $GFP_{515\text{-}575\ nm}$, $dsRed_{575\text{-}650\ nm}$, $Cy5.5_{695\text{-}770\ nm}$ and $ICG_{810\text{-}885\ nm}$ emission bandpass filters included in these settings accurately overlap with the spectra of the dyes (**Figure 2A**). Against a black background, SBRs obtained with FITC were the highest, followed by TRITC, ICG and finally Cy5.5 (**Figure 2B**). At a concentration 0.2 and 0.5 mg/mL most dyes reached maximal brightness. At concentrations higher than 0.5 mg/mL the signals maximized and started to decrease which is probably due to self-absorption. For example, for ICG we found a curve that directly corresponds to the findings of Mordon et al. [18]. We chose a standard dye concentration of 0.5 mg/mL for further (tissue penetration) experiments, since at this concentration all dyes showed emission intensities close to their maximum.

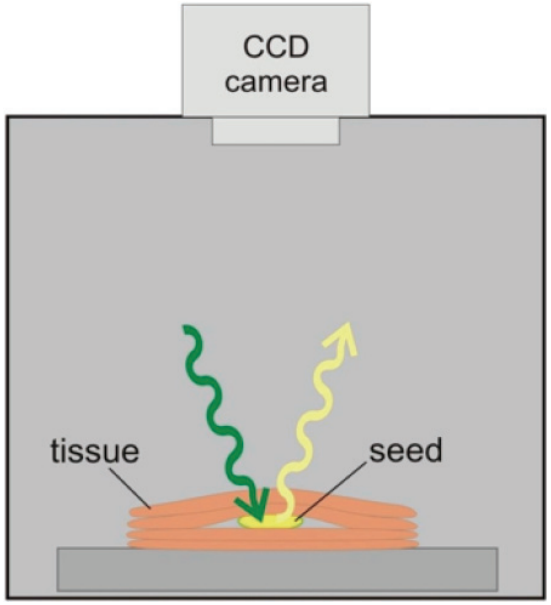


Figure 1. Experimental setup. A glass seed containing a luminophore (or a combination of several) is placed on a ~4 mm layer of tenderloin/sirloin/lard in the imaging chamber of the IVIS 200 system. After taking a picture of the bare seed, it is then covered with layers of tissue and imaged at every step.

Organic dyes: tissue penetration

To measure the tissue penetration, dye-containing glass seeds were imaged covered with increasing amounts of tenderloin tissue. Against a background of pork tenderloin, the highest SBR was again obtained with FITC (43), followed by Cy5.5 (26), and finally TRITC and ICG, who had roughly the same SBR (10 resp. 8; **Figure 2C**).

When covered with tissue, the FITC signal became undetectable 3-4 mm, while TRITC was visible up to about 6 mm. Both Cy5.5 and ICG signals could be detected through 14 mm of tissue (**Figure 2C**). Tissue penetration increased with an increase in excitation and emission

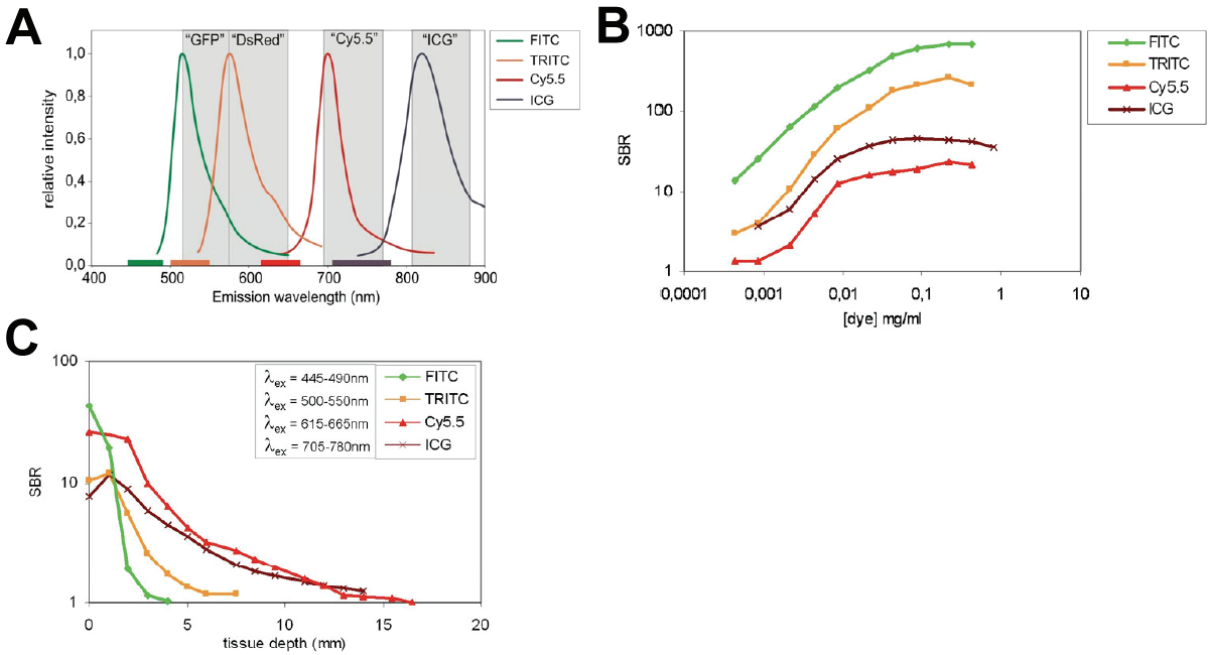


Figure 2. Luminescent characteristics of organic dyes. A) Spectra for FITC, TRITC, Cy5.5 and ICG (peaks normalized to 1) and relevant IVIS 200 emission filter bands (resp. $GFP_{515\text{-}575\ nm}$, $dsRed_{575\text{-}650\ nm}$, $Cy5.5_{695\text{-}770\ nm}$ and $ICG_{810\text{-}885\ nm}$ settings). The excitation filter bands are depicted as bars on the x-axis, with the colors matching those of the dyes in the graph. B) Concentration curve: Comparison of luminescence intensities of all dyes at different concentrations. C) Tissue penetration of 0.5 mg/mL organic dye in a marker seed covered by tenderloin, measured as mentioned in A). Excitation wavelength filters were added to the legend. The lower initial SBR's found in (C), relative to (B) is a result of the underlying piece of tissue that is only present in (C; see Figure 1)).

wavelengths, while Cy5.5 and ICG were equally capable of penetrating the tenderloin tissue. Of note, the graphs for TRITC and ICG both showed an increase in SBR between 0 and 2 mm of overlying tissue depth, which appears to be caused by placing the first layer of tissue on top of the marker seed. After this initial rise in SBR, the SBR started to decline. This effect might be caused by the alteration of the scattering and reflection properties related to the placement of tissue on top of the marker seed, which may have changed the fraction of the emitted signal reaching the camera.

InP/ZnS quantum dots

To compare the tissue penetration of different exciton emissions (excited at the same wavelength), we studied two types of dual emissive InP/ZnS QDs, one with a 565nm λ_{max} (green) and one with a 630nm λ_{max} (red) exciton emission. Both QD versions were imaged using the "GFP" excitation filter (**Figure 3A**). The green QD emission was detected using the corresponding $GFP_{515\text{-}575\ nm}$ emission band pass filter. For the red QDs the best emission filter would be the $dsRed_{575\text{-}650\ nm}$ one, but unfortunately the IVIS 200 does not allow the combination of "GFP" excitation (445-490 nm) and $dsRed_{575\text{-}650\ nm}$ emission filters. The highest SBR with these QDs was found with "GFP" excitation plus a standard "660" (650-670 nm) emission filter (**Figure 3A**).

InP/ZnS quantum dots: signal vs. concentration

The concentration curves (mg/mL) show that InP/ZnS QDs have a much lower SBR compared to organic dyes: at 0.5 mg/mL the signal was less than 2 times higher than the (black) background signal, while with all organic dyes a SBR of >20 was obtained at a similar concentration (**Figure 3B**). To aquire a comparable signal intensity in the tissue penetration experiments and allow for comparison with organic dyes, we used seeds with two concentrations of QDs; 1 mg/mL and 10 mg/mL (**Figure 3C**). Against a background of tenderloin tissue, a poor SBR was obtained for the 1mg/mL seeds. At 10 mg/mL the SBR of the 630 nm exciton emission of

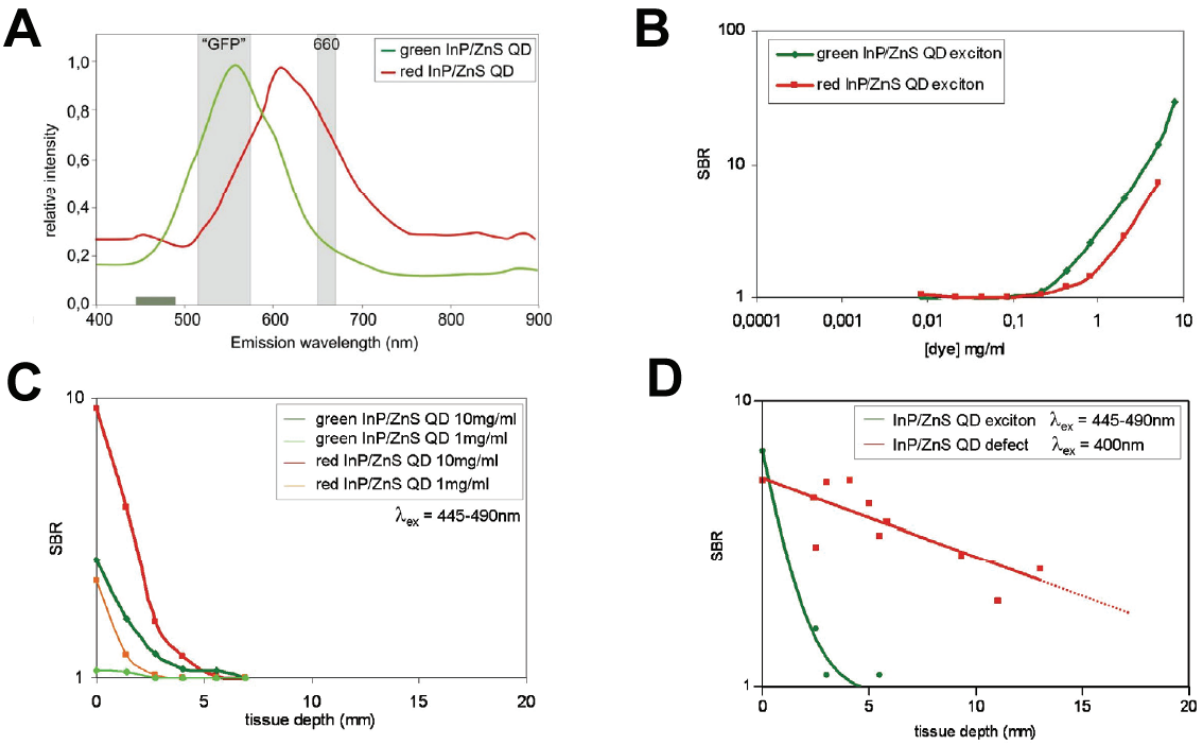


Figure 3. Luminescent characteristics of two InP/ZnS QDs. A) Spectra of exciton emissions (peaks normalized to 1) and relevant IVIS 200 emission filter bands (resp. $GFP_{515\text{-}575\ nm}$ and 660 nm). The GFP excitation filter band is depicted as a gray bar on the horizontal axis. B) Concentration curve: Comparison of luminescence intensities of the two different QDs at different concentrations. C) Tissue penetration of 1 mg/mL and 10 mg/mL green and red QDs in a marker seed covered by tenderloin, measured using the IVIS 200 GFP excitation + $GFP_{515\text{-}575\ nm}$ emission setting (green QD) or a combination of GFP excitation + 660 nm emission settings (red QD). D) Comparison of tissue penetration of InP/ZnS QD exciton and defect emissions. Figure 4D is adapted from Chin et al. (2009) [13]. The lower initial SBR's found in (C), relative to (B) is a result of the underlying piece of tissue that is only present in (C; see Figure 1)).

red QDs was comparable to that of 0.5 mg/mL TRITC and ICG (roughly SBR 10; **Figures 2C** and **3C**). In contrast the SBR of the 565 nm exciton emission of green QDs at 10 mg/mL was a mere 2.4.

InP/ZnS quantum dots: tissue penetration

The tissue penetration of the green QDs exciton emission was about 3 mm, much like FITC. The red QD exciton emission could be seen up to 4 mm (**Figure 3C**), which was hardly more than FITC (excited at the same wavelength, 445-490 nm), less than TRITC and far less than Cy5.5 (excited at 500-550 nm, respectively 615-665 nm), despite its emission maximum of 630 nm, which lies in between that of TRITC and Cy5.5. Compared to the exciton emission of the QDs, which was elicited by real time excitation with blue light, the pre-illuminated QD defect emission (λ_{em} =650 nm) showed significantly higher tissue penetration (**Figure 3D**). For green QDs, whose exciton emission only reached 3-4 mm, the defect emission could be seen up to 14 mm, which is comparable to the best performing organic dyes, Cy5.5 and ICG (**Figures 2C** and **3D**).

Comparison of quantum yields

Multiplying the quantum yields known for the luminophores (FITC ~90 % [19], TRITC ~35 % [20], Cy5.5 ~23 % [21], ICG ~1,3 % [22], QDs ~70 % [13]) with the molar concentrations used in our experiments revealed that seeds containing FITC emitted the highest number of photons/s. TRITC, Cy5.5 and ICG emitted roughly 33 %, 10 % and 1 %, respectively, of the light emitted by FITC. The QDs emitted an amount of light comparable to ICG (~1 % of FITC), although

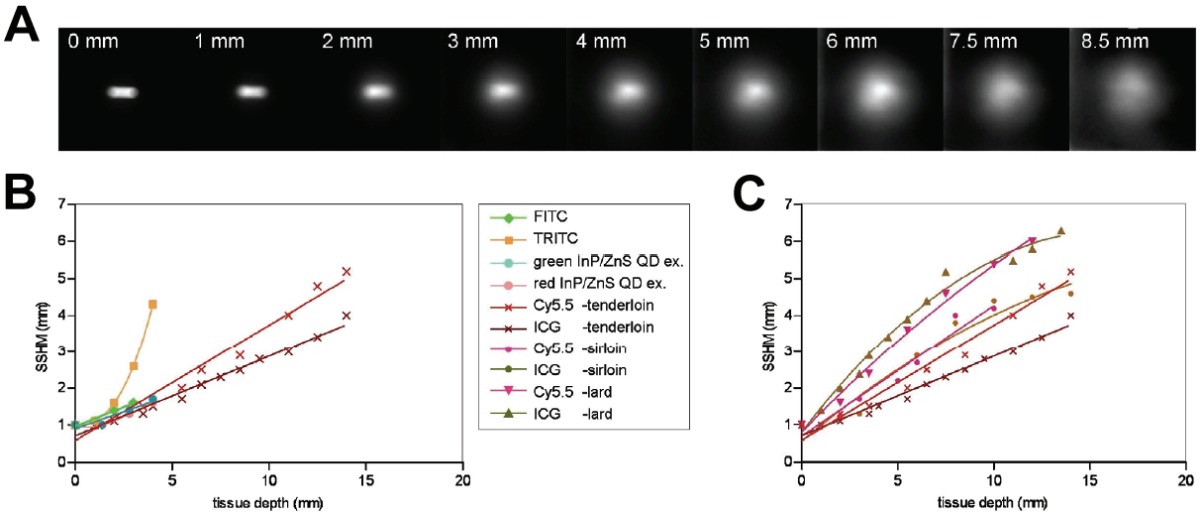


Figure 4. Signal scattering. A) Example of signal scatter of an ICG-containing seed: The uncovered seed (0 mm) gives a signal comparable to the actual size of the seed, while covering the seed with layers of tenderloin tissue increases the diameter of the signal (1-8.5 mm). B) Signal scatter for ICG, Cy5.5 and InP/ZnS QDs covered by tenderloin, determined from the same images as Figures 2C and 3C. C) Signal scatter for ICG and Cy5 in tenderloin, sirloin and lard, determined from the same measurements as used for Figures 2C and 4C-D.

this is a rough estimate, since the size and thus the molecular weight of the QDs present in the solution varies [23].

Signal scattering

Scattering of the luminescent signal leads to loss of resolution. Not only can scattering make it impossible to distinguish two seeds that are close together, but it can also make a small but bright light-source situated deep within the tissue appear the same as a large but dim light-source situated just under the surface (see **Figure 4A** for an example).

Measuring the SSHM of organic dyes and QDs in glass seeds, we found that in tenderloin the signal diameter of most luminophores increased almost linearly with increasing tissue depth (**Figure 4B**). For both ICG and Cy5.5 the diameter of the signal increased to >4 times the size of the marker seed before the signal was lost at around 14 mm tissue depth. The effect of scattering on the FITC and both green- and red InP/ZnS QD emissions was similar to that of Cy5.5 and ICG (although at shallower depths). Only the TRITC signal seemed to suffer more from scattering. For TRITC the signal diameter had already increased >4-fold at 4 mm tissue depth, which is only 67 % of its maximum penetration.

To compare scattering in different tissues we also determined the SSHM for ICG and Cy5.5 in sirloin and lard (**Figure 4C**). Here we found that for both dyes the scattering was higher in lard than in tenderloin, while in sirloin the scatter was not significantly higher than in tenderloin. However, in tenderloin Cy5.5 seemed to be affected by scattering slightly more than ICG. In sirloin and lard the two dyes were scattering occurred to the same extent.

Background signal of different organs

When choosing an appropriate dye for a specific application, it is also important to know the background signal of the organs, at the relevant excitation/emission wavelengths, in which it will be used. For this reason background signals were determined by correcting for of tissue autofluorescence and reflection of the excitation light (**Figure 5A**). Also, background signals caused by the sirlion, tenderloin and lard were determined (**Figure 5B**).

In **Figure 5A** can be seen that for pale (mouse) tissues, such as brain, fat and muscle, the background signal is highest in the $GFP_{515\text{-}575\ nm}$ channel, followed by the $dsRed_{575\text{-}650\ nm}$, $Cy5.5_{695\text{-}770\ nm}$ and $ICG_{810\text{-}885\ nm}$ settings. This was also the case for the 'pale' tenderloin and

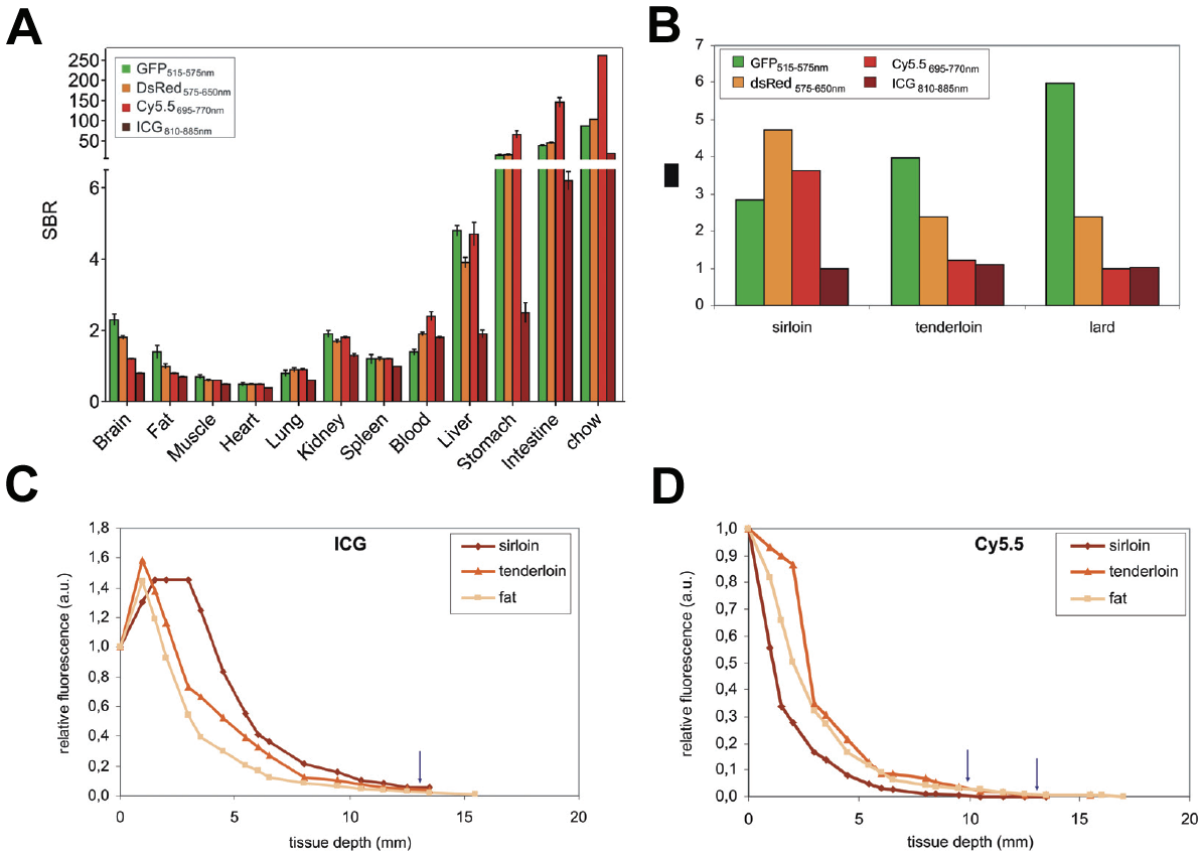


Figure 5. Background luminescence and tissue-dependent penetration. A) Background luminescence of different mouse organs, measured on the IVIS 200 system, using the $GFP_{515\text{-}575\ nm}$, $dsRed_{575\text{-}650\ nm}$, $Cy5.5_{695\text{-}770\ nm}$ and $ICG_{810\text{-}885\ nm}$ settings. B) Background luminescence of tenderloin, sirloin and lard, measured as in A. C) Tissue penetration of ICG in bloody tissue (sirloin), pale tissue (tenderloin) and fat (lard). SBR values were normalized to the value for a bare seed. D) Tissue penetration of Cy5.5 in bloody tissue (sirloin), pale tissue (tenderloin) and fat (lard). Relative fluorescence values were normalized to the value for a bare seed. The blue arrows indicate the tissue depth at which the signal is lost.

fat representing lard (**Figure 5B**). In contrast, for mouse blood the $GFP_{515\text{-}575\ nm}$ channel gave the lowest signal, followed by $ICG_{810\text{-}885\ nm}$ and $dsRed_{575\text{-}650\ nm}$, with a maximum in the $Cy5.5_{695\text{-}770\ nm}$ channel. The dark red mouse tissues like liver and spleen, but also the sirloin tissue (more blood-containing), showed a pattern that is intermediate of mouse blood and pale tissues. Note that in general the ratio of $ICG_{810\text{-}885\ nm}$ and $Cy5.5_{695\text{-}770\ nm}$ signals are similar, except for mouse liver, stomach and intestine. In stomach and intestines the background signal was much higher overall, but especially strong in the $Cy5.5_{695\text{-}770\ nm}$ channel. These two organs contain the non-specialized chow the animals were given, which was highly autofluorescent (**Figure 5A**).

Tissue dependent penetration

For ICG, the tissue penetration depths in sirloin, tenderloin and lard were comparable, since in all cases the signal was lost after ~14 mm (**Figure 5C**). For Cy5.5 the penetration through sirloin was less efficient, as the signal was undetcable at 10 mm in sirloin compared to roughly 14 mm in tenderloin and lard (**Figure 5D**). Consequently, ICG slightly outperforms Cy5.5 in tissues with a high blood-content.

Dye mixtures for multispectral signal-depth estimation

Previously we have shown that multispectral imaging of dual-emissive InP/ZnS QDs can be

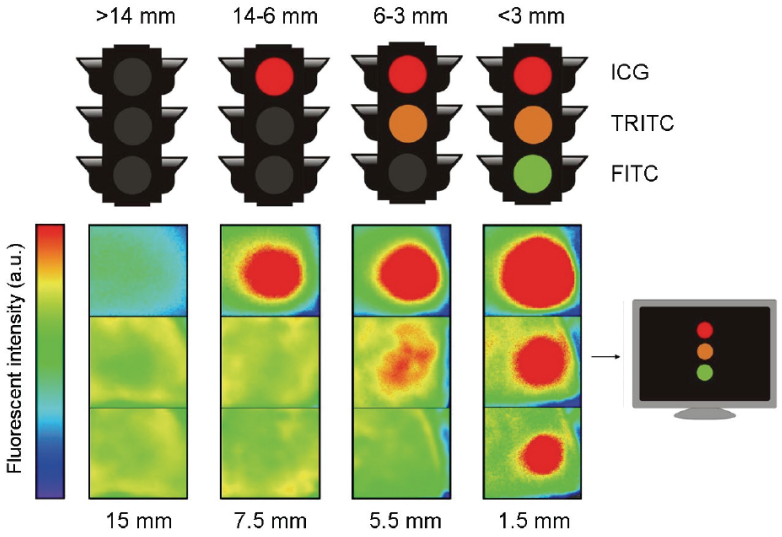


Figure 6. Traffic light analogue for depth estimation using a marker seed filled with a mixture of ICG, TRITC and FITC. Depending on how many colors of the traffic light can be detected, an estimation of depth can be made (top illustration). A camera system is required to detect the ICG signal and can aid in visualizing the TRITC and FITC signals; Here the IVIS 200 $ICG_{810\text{-}885\ nm}$, $dsRed_{575\text{-}650\ nm}$ and $GFP_{515\text{-}575\ nm}$ settings were used, and the signal intensities are shown using the standard (reversed) Rainbow color table. TRITC and FITC can also be seen by eye and the perceived color of the dye mixture provides a direct indication of depth.

used to estimate the signal depth [1]. By adding a third emission, this depth estimation approach could be further fine-tuned. FITC and ICG were combined in one seed together with TRITC, which was added because its tissue penetration depth lies between that of FITC and ICG (**Figure 2C**). As Cy5.5 and ICG behaved so similar in the tissue penetration experiments described above, Cy5.5 was omitted from these experiments.

Mixed together, the three dyes behaved much like they did in separate seeds, thereby yielding a so called inverted "traffic light". To illustrate this concept, **Figure 6** shows the signals detected at 4 different depths chosen to fall either completely outside, or inside the depth penetration range of one or more dyes: Using the IVIS 200, no signal could be detected at 15 mm; at 7.5 mm only ICG could be observed; at 5.5 mm both the ICG and TRITC signals were visible and at 1.5 mm the FITC signal could be detected as well. Hence the more colors that can be observed simultaneously, the closer one is to the marker seed. While a camera is required to detect NIR dyes like ICG, lower wavelength dyes like FITC and TRITC can be seen by eye when excited with UV/blue light: When approaching the seed, first the red TRITC signal can be seen, followed by an increasingly orange/yellow signal resulting from a mixture of TRITC and FITC emissions.

Discussion

Using multispectral imaging, a combination of visible and NIR emissions can be used to determine the depth of the marker seed based on the characteristics of each individual dye. To improve the translational nature of the "traffic light" approach for the visualization of surgical safety margins, the potential of multi-emissive marker seeds containing organic dyes was determined. By combining the organic dyes FITC, TRITC and ICG in a single marker seed, the multispectral fluorescence imaging procedure by adding an additional step in the detection process could be refined. Where previously two signals could be discriminated [1], now four depth ranges could be distinguished (no signal (>14 mm), just ICG (range 6-14 mm), ICG+TRITC (range 3-6 mm) and ICG+TRITC+FITC (<3 mm)). Clearly any increase of detail regarding the surgical safety margins can be considered beneficial for the intraoperative decision making procedure.

In our experiments the concentration curves of the organic dyes adequately reflected the differences in quantum yield. Because the quantum yield is based on the molar concentration and QDs have a much higher molecular weight, the concentration curve of the QDs could not be directly compared to those of the organic dyes. In any case, the differences in quantum yield did not directly correlate with tissue penetration depth. The dye with the highest quantum yield (FITC) had the lowest tissue penetrating capacity and vice versa. This shows that differences in excitation and emission wavelength maximum have a much stronger impact on tissue penetration than the quantum yield.

The tissue penetration depth is influenced by

tissue attenuation (absorption plus scattering) as well as the height of the background signal. Although we did not measure the absorption for the different tissues directly, absorption of both the excitation and emission signals can account for most of the differences we observed between the different luminescent emissions.

For traditional organic dyes, the difference between the absorption and emission maximum (the Stokes shift) is usually less than 50 nm, while for luminescent nanoparticles this difference may be much larger [25]. However, QDs typically reveal a very small stokes shift in reference to their absorbance onset. Only a sufficient QD absorbance which is comparable to organic dyes at their absorbance maximum is often found to be far blue shifted with respect to the QD absorbance onset. In our experiments the 630 nm-emitting InP/ZnS QDs performed just as poorly as the 565 nm-emitting ones, despite their more favorable emission wavelength, suggesting that a sufficient absorption of the 445-490 nm excitation light is the limiting factor in QD imaging. This is in accordance with our observation that the pre-illuminated 660 nm defect emission does yield a tissue penetration, similar to Cy5.5 and ICG.

The similarity in tissue penetration (<1.5 cm) of emissions >650 nm lead us to suspect that a sort of "cut-off wavelength" exists at around 650 nm. Dyes with emissions at shorter wavelengths have clearly inferior tissue penetration. It should also be noted that the maximum penetration depths reported here are based on a SBR which was only slightly more than 1. This value may be a somewhat optimistic value for surgical guidance applications.

In a similar degree, scattering seemed to affect the tissue attenuation of most dyes. This effect is wavelength-dependent, with shorter wavelengths showing a higher degree of scattering than longer wavelengths [24]. In tenderloin we indeed found that TRITC is scattered more than Cy5.5, and Cy5.5 shows slightly more scattering than ICG. For FITC and the QDs we did not find strong scattering properties, possibly because scattered short-wavelength light is completely absorbed by the tissue. Still, scattering may have contributed to the strong signal attenuation of luminophores emitting (or excited) at shorter wavelengths.

In addition to tissue attenuation, we found that the background signal in different organs and tissue types was wavelength dependent. A shift from mostly green luminescence in pale tissues to more red-containing luminescence in dark tissues (with a higher blood-content) was observed. The relatively high background signal in the $Cy5.5_{695\text{-}770\ nm}$ channel, and to a lesser extent also in the $ICG_{810\text{-}885\ nm}$ channel, is most likely related to reflection of the imperfectly filtered excitation light. Never the less, Cy5.5 seemed to have favorable optical properties that are similar to those of ICG.

Of course we realize that we only investigated a limited number of tissues types and that one might encounter more variations during an actual clinical procedure [26]. On top of that, the flat shape of the phantom tissue may also positively influence the penetration depth. However, we do believe that the phantom experiments that we performed illustrate a trend that might also be of value in a clinical setting.

Regarding the criteria for choosing luminophores, we have seen that organic dyes could be used at low concentrations, while a much higher concentration of QDs was needed to achieve an acceptable SBR. The tissue penetration capacity of organic dyes was dependent on their emission wavelength maximum and was quite high for (infra) red dyes. In contrast, the strong attenuation of the UV/blue excitation light caused poor tissue penetration of InP/ZnS QD exciton emissions and limited their use in superficial imaging. Optimizing the excitation by using a specialized high-intensity 400 nm light-source may yield improvements, but such modifications will also reduce the chance of a clinical translation.

Although the tissue penetration of the defect emission from InP/ZnS QDs was considerably better, it was also markedly less bright, necessitating both a higher concentration and much longer camera exposure time of over 2 minutes. Organic dyes proved to be a good alternative for dual-emissive QDs. A clinical application in which this traffic light concept might be of use is in breast conserving surgery, where the surgeon wants to know, while executing the excision, whether he/she is approaching the tumor and if he/she is keeping a sufficient safety margin of at least 2 mm [27].

We have demonstrated previously that such a traffic-light approach would be most beneficial

in a multimodal setting whereby a 3D modality helps guide the surgeon towards the marker seed [1]. Our clinical experience with surgical fluorescence guidance, furthermore, demonstrates that integrating e.g. gamma-tracing with fluorescence imaging improves the intraoperative detection rate compared to using fluorescence guidance alone [26].

Conclusions

In designing and choosing luminophores for possible surgical applications, several criteria should be considered. The poor compatibility with clinical modalities combined with their possible toxicity may limit the future translation of QDs to the clinic. The equal or superior optical properties of organic dyes, combined with low toxicity and easy detection, makes these more practical for clinical translation. By combining multiple organic dyes in a marker seed approach we have further optimized our traffic light based depth estimation approach.

Acknowledgements

This research is supported, in part, by a NWO-VENI grant (PC) and a KWF-translational research award (Grant No. PGF 2009-4344; FvL).

Address correspondence to: Dr. van Leeuwen FWB, Department of Radiology Interventional Molecular Imaging, Leiden University Medical Center (LUMC), Albinusdreef 2, PO Box 9600, postzone C2-S, 2300 RC, Leiden, The Netherlands Tel: +31(0)71 526 3491; Fax: +31(0)71 5248256; E-mail: F.W.B.van_Leeuwen@LUMC.nl

References

[1] Buckle T, Chin PTK, van den Berg NS, Loo CE, Koops W, Gilhuijs KG, van Leeuwen FWB. Tumor bracketing and safety margin estimation using multimodal marker seeds: a proof of concept. J Biomed Opt 2010; 15: 56021-56028.

[2] Terasaki H, Miyake Y, Awaya S. Fluorescein angiography of peripheral retina and pars plana during vitrectomy for proliferative diabetic retinopathy. Am J Ophthalmol 1997; 123: 370-376.

[3] Alsagoff Z, Chew PTK, Chee CKL, Wong JS, Aung T. Indocyanine green anterior segment angiography for studying conjunctival vascular changes after trabeculectomy. Clin Experiment Ophthalmol 2001; 29: 22-26.

[4] Tagaya N, Yamazaki R, Nakagawa A, Abe A, Hamada K, Oyama T. Intraoperative identification of sentinel lymph nodes by near-infrared fluorescence imaging in patients with breast cancer. Am J Surg 2008; 195: 850-853.

[5] Kitai T, Inomoto T, Miwa M, Shikayama T. Fluorescence navigation with indocyanine green for detecting sentinel lymph nodes in breast cancer. Breast Cancer 2005; 12: 211-215.

[6] Motomura K, Inaji H, Komoike Y, Hasegawa Y, Kasugai T, Noguchi S, Koyama H. Combination technique is superior to dye alone in identification of sentinel node in breast cancer patients. J Surg Oncol 2001; 76: 95-99.

[7] Ntziachristos V. Going deeper than microscopy: the optical imaging frontier in biology. Nat Methods 2010; 7: 603-614.

[8] Weissleder R, Ntziachristos V. Shedding light onto live molecular targets. Nat Med 2003; 9: 123-128.

[9] Frangioni JV. In vivo near-infrared fluorescence imaging. Curr Op Chem Biol 2003; 7: 626-634.

[10] Zhou L, El-Deiry WS. Multispectral fluorescence imaging. J Nucl Med 2009; 50: 1563-1566.

[11] Stevenson RM, Mansfield JR. Multispectral imaging in biology and medicine: slices of life. Cytometry part A 2006; 69A: 748-758.

[12] Levenson RM, Lynch DT, Kobayashi H, Backer JM, Backer MV. Multiplexing with multispectral imaging: from mice to microscopy. ILAR J 2008; 49: 78-88.

[13] Chin PTK, Buckle T, Aguirre de Miguel A, Meskers SCJ, Janssen RAJ, van Leeuwen FWB. Dual-emissive quantum dots for multispectral intraoperative fluorescence imaging. Biomaterials 2010; 31: 6823-6832.

[14] Klimov VI, Mikhailovsky AA, Xu S, Malko A, Hollingsworth JA, Leatherdale CA, Eisler H, Bawendi MG. Optical Gain and Stimulated Emission in Nanocrystal Quantum Dots. Science 2000; 290: 314-317.

[15] Hardman RA. Toxicologic Review of Quantum Dots: Toxicity Depends on Physicochemical and Environmental Factors. Environ. Health Perspect 2006; 114: 165-172.

[16] Biju V, Itoh T, Anas A, Sujith A, Ishikawa M. Semiconductor quantum dots and metal nanoparticles: syntheses, optical properties, and biological applications. Anal Bioanal Chem 2008; 391: 2469-2495.

[17] Shao F, Yuan H, Josephson L, Weissleder R, Hilderbrand SA. Facile synthesis of monofunctional pentamethine carbocyanine fluorophores. Dyes Pigments 2011; 90: 119-122.

[18] Mordon S, Devoiselle JM, Soulie-Begu S, Desmettre T. Indocyanine Green: Physicochemical Factors Affecting Its Fluorescence in Vivo. Microvasc Res 1998; 55: 146-152.

[19] Hungerford G, Benesch J, Manob JF, Reisb RL. Effect of the labelling ratio on the photophysics of fluorescein isothiocyanate (FITC) conjugated to bovine serum albumin. Photochem. Photobiol Sci 2006; 6: 152-158.

[20] Whitaker JE, Haugland RP, Ryan D, Hewitt PC, Haugland RP, Prendergast FG. Fluorescent

rhodol derivatives: versatile, photostable labels and tracers. Anal Biochem 1992; 207: 267-279.
[21] Mujumdar SR, Mujumdar RB, Grant CM, Waggoner AS. Cyanine-labeling reagents: sulfobenzindocyanine succinimidyl esters. Bioconjug Chem 1996; 7: 356-362.
[22] Benson RC, Kues HA. Fluorescence properties of indocyanine green as related to angiography. Phys Med Biol 1978; 23: 159-163.
[23] Kim S, Lim YT, Soltesz EG, De Grand AM, Lee J, Nakayama A, Parker JA, Mihaljevic T, Laurence RG, Dor DM, Cohn LH, Bawendi MG, Frangioni JV. Near-infrared fluorescent type II quantum dots for sentinel lymph node mapping. Nat Biotechnol 2003; 22: 93-97.
[24] Matcher SJ, Cope M, Delpy DT. In vivo measurements of the wavelength dependence of tissue-scattering coefficients between 760 and 900 nm measured with time-resolved spectroscopy. Appl Opt 1997; 36: 386-396.
[25] Resch-Genger U, Grabolle M, Cavaliere-Jaricot S, Nitschke R, Nann T. Quantum dots versus organic dyes as fluorescent labels. Nat Methods 2008; 5: 763-775.
[26] van der Poel HG, Buckle T, Brouwer OR, Valdés Olmos RA, van Leeuwen FWB. Intraoperative laparoscopic fluorescence guidance to the sentinel lymph node in prostate cancer patients; clinical proof of concept of an integrated functional imaging approach using a multimodal tracer. Eur Urol 2011; 60: 826-833.
[27] Pleijhuis RG, Langhout GC, Helfrich W, Themelis G, Sarantopoulos A, Crane LM, Harlaar NJ, de Jong JS, Ntziachristos V, van Dam GM. Near-infrared fluorescence (NIRF) imaging in breast-conserving surgery: Assessing intraoperative techniques in tissue-simulating breast phantoms. Eur J Surg Oncol 2011; 37: 32-39.